

Validation of MODIS-based Annual Actual Evapotranspiration against Water Balance Estimates in Murray-Darling Basin

Zhang Y.Q.¹, F.H.S Chiew¹, L. Zhang¹, H. A. Cleugh² and R. Leuning²

¹ CSIRO-Land and Water, GPO BOX 1666, Canberra ACT 2601, Australia,

² CSIRO- Marine and Atmospheric Research GPO BOX 1666, Canberra ACT 2601, Australia

Email: yongqiang.zhang@csiro.au

Keywords: *Evapotranspiration, remote sensing, MODIS, Penman-Monteith, surface conductance model*

EXTENDED ABSTRACT

Estimates of actual evapotranspiration (ET) are important for understanding regional water balance, irrigation requirements, atmospheric boundary layer stability and weather forecasting. However, it is difficult to measure ET directly, and in most applications ET is estimated using models.

Remotely sensed (RS) data provide an opportunity for estimating spatially distributed ET (ET_{RS}) directly. The MODERate resolution Imaging Spectrometer (MODIS) data are commonly with ET models to estimate ET_{RS} , because of its high radiometric sensitivity, high temporal resolution and moderate spatial resolution, and it is free of charge.

ET_{RS} is usually validated at point locations against micro-meteorological measurements, such as Bowen-ratio energy balance and eddy-covariance system. These point validation can evaluate the temporal variation of ET, but cannot assess the spatial pattern of ET. A few attempts have been made to validate ET_{RS} against catchment scale ET estimates based on water balance (Bastiaanssen *et al.* 2005). However, the validation is carried out in 1-2 catchments in a period of 1 year.

This study assesses mean annual ET_{RS} estimates against water balance estimates at 76 catchments in Murray-Darling Basin (MDB) in the periods of 2001-05. The ET_{RS} is estimated using the Penman-Monteith equation combined with a new surface conductance model for 1 x 1 km² grids across the MDB. The inputs to the model are mainly MODIS leaf area index and land classification data and gridded meteorological data. In this study, the five parameters in the surface conductance model are calibrated, separately for three climatic regions (humid, semi-arid and arid).

The results indicate that the MODIS-based Penman-Monteith approach used here can

satisfactorily estimate catchment scale ET. The results also suggest that the approach can reasonably estimate catchment runoff. This is particularly interesting because the approach is relatively simple and can provide spatial coverage of ET (and runoff) across entire regions of interest (e.g. entire Murray-Darling Basin or Australia).

It is likely that the approach used here and other remote sensing based ET methods can be used together with rainfall-runoff models (either to constrain rainfall-runoff model estimates or to improve rainfall-runoff model calibration, parameterization and regionalisation) to improve runoff predictions in ungauged catchments.

1. INTRODUCTION

Estimates of land surface evapotranspiration (ET) are important for the understanding regional or catchment water balance, irrigation water requirements, atmospheric boundary layer stability and weather forecasting. Owing to spatial continuity, remotely sensed (RS) data are often used to drive models to estimate spatially distributed ET (ET_{RS}). The Terra/MODerate Resolution Imaging Spectrometer (MODIS) satellite data are commonly used together with ET models to estimate ET_{RS} (Cleugh *et al.* 2007, Leuning *et al.* 2007, Zhang and Wegehenkel 2006). This is because MODIS, flying aboard NASA's TERRA and AQUA satellites, is high radiometric sensitive with high temporal resolution and moderate spatial resolution, and it is free of charge.

The validation of ET_{RS} is generally conducted at point/plot scale by using measurements from eddy-covariance or Bowen-ratio energy balance methods. The point ET validation can evaluate the temporal variation of ET_{RS} , but it cannot assess spatial patterns of ET_{RS} . Some attempt has been made to validate ET_{RS} against catchment scale estimates of ET based on water balance (Bastiaanssen *et al.* 2005), which, however focuses on only several catchments.

This paper assesses MODIS-based ET_{RS} estimates against water balance ET estimates from 76 catchments in Murray-Darling Basin. The mean annual ET estimates, averaged over 2001-2005, are assessed. Because the water storage change in a catchment is small relative to the rainfall and ET over several years, ET_{RS} can be directly compared with water balance ET estimates derived from long-term rainfall minus long-term runoff. The paper also provides a direct indication of the potential use of ET_{RS} as an estimate of long-term runoff in ungauged catchments or to constrain rainfall-runoff modeling parameterization.

2. ET ESTIMATES FROM LONG-TERM CATCHMENT WATER BALANCE (ET_{WB})

Catchment scale ET can be estimated from water balance over timescales where catchment water storage changes are negligible. Over a long period (e.g., 5-10 years), large-scale catchment water balance for an undisturbed catchment can be written as:

$$ET_{WB} = P - R \quad (1)$$

Where ET_{WB} is catchment scale ET, P is precipitation, and R is total runoff from the

catchment measured by a gauging station at the catchment outlet.

The streamflow data required to estimate ET_{WB} are obtained from dataset compiled for the Australian Land and Water Resources Audit Project (Peel *et al.*, 2000). Data from 76 unimpaired catchments with catchment areas varying in 50-2000 km² were used to validate ET_{RS} because it is easily to aggregate 1 × 1 km² grid ET_{RS} to catchment ET_{RS} when catchment area is over 50 km².

3. ET ESTIMATES FROM MODIS USING THE PENMAN-MONTEITH APPROACH

3.1. Leaf Area Index based Penman-Monteith approach

ET_{RS} is estimated using the Penman-Monteith (P-M) equation combined with a surface conduction (G_s) model in which G_s is estimated from leaf area index (LAI). The P-M equation can be written as:

$$ET_{RS} = \frac{1}{\lambda} \frac{\Delta(R_n - G) + \rho_a C_p D G_a}{\Delta + \gamma(1 + G_a / G_s)} \quad (2)$$

where λ is the latent heat of vaporization, $\Delta = de^*/dT_a$, is the slope of the curve relating saturation water vapour pressure to temperature, $D = e^*(T_a) - e_a$ is the vapour pressure deficit of the air, $e^*(T_a)$ is the saturation vapour pressure at a given air temperature, e_a is the actual vapour pressure, γ is the psychrometric constant, ρ_a is the air density, C_p is the specific heat capacity of air, R_n is the net radiation, and G is the soil heat flux.

The net radiation (R_n) is calculated as the difference between the incoming net short-wave radiation (R_{ns}) and the outgoing net long-wave radiation (R_{nl}):

$$R_n = (R_{ns} - R_{nl}) \quad (3)$$

R_{ns} equals to $(1 - \alpha_c)R_s$, where α_c is the surface albedo and R_s is solar radiation. R_{nl} is calculated using the method of Allen *et al.* (1998):

$$R_{nl} = \sigma \left[\frac{T_{\max}^4 + T_{\min}^4}{2} \right] \left(0.34 - 0.14 \sqrt{e_a} \right) \left(1.35 \frac{R_s}{R_{so}} - 0.35 \right) \quad (4)$$

where σ is the Stefan-Boltzmann constant (4.903×10^{-9} MJ/K⁴/m²/d), T_{\max} is the maximum air temperature in Kelvin, T_{\min} is the minimum air temperature in Kelvin, R_{so} is clear-sky solar

radiation, and R_s/R_{s0} is the relative shortwave radiation (limited to ≤ 1.0).

G is assumed as a proportion (a_1) of the net radiation:

$$G = a_1 R_n \quad (5)$$

a_1 is set to 0.1 based on measurements at savanna sites (Cleugh *et al.* 2007).

The aerodynamic conductance (G_a) in this study is assumed to be a constant for each vegetation type [due](#) to lack of measured wind speed data:

$$G_a = \begin{cases} 1/30 & \text{forests} \\ 1/80 & \text{shrubs} \\ 1/100 & \text{grasslands and cropland} \end{cases} \quad (6)$$

This approximation should not significantly affect ET estimates as the P-M equation is not sensitive to variation of aerodynamic conductance when it is in the range of 1/30 - 1/100 s/m (Zhang and Dawes 1995).

Amongst the variables of the P-M equation, G_s is the only variable dependent on vegetation physiological characteristics. A new G_s model developed by Leuning *et al.* (2007) is used here. The main developments of the new G_s approach is that (1) a non-linear relationship between LAI and canopy conductance instead of the linear one of Cleugh *et al.* (2007) is used, and (2) the fraction of equilibrium evaporation at soil surface f (varying between 0 to 1) is appended into the G_s model. Leuning *et al.* (2007) showed that:

$$G_s = G_c \left[\frac{1 + \frac{\tau G_a}{(1 + \varepsilon) G_c} \left[f - \frac{(\varepsilon + 1)(1 - f) G_c}{G_a} \right] + \frac{G_a}{\varepsilon G_i}}{1 - \tau \left[f - \frac{(\varepsilon + 1)(1 - f) G_c}{G_a} \right] + \frac{G_a}{\varepsilon G_i}} \right] \quad (7)$$

$$G_c = \frac{g_{sx}}{k_Q} \ln \left[\frac{Q_h + Q_{50}}{Q_h \exp(-k_Q \text{LAI}) + Q_{50}} \right] \left[\frac{1}{1 + \frac{D}{D_0}} \right] \quad (8)$$

where ε is Δ/γ , $G_i = \gamma(R_n - G)/(\rho_a C_p D)$ is the isothermal conductance (Monteith and Unsworth 1990), G_c is canopy conductance, $\tau = \exp(-k_A \text{LAI})$ is the fraction of available energy transmitted downward at LAI, g_{sx} is the maximum stomatal conductance, k_Q is the extinction coefficient for photosynthetically active radiation, k_A is the attenuation of net all-wave irradiance, Q_h is the photosynthetically active radiation at the top of canopy, Q_{50} is the value of

absorbed photosynthetic active radiation when stomatal conductance $g_s = g_{sx}/2$ (g_{sx} is the maximum value of g_s), D_0 is the value of D when the stomatal conductance is reduced $g_{sx}/2$.

To calculate ET_{RS} , we should get metrological (minimum air temperature, maximum air temperature, vapor pressure and solar radiation), LAI and land classification data and optimize the six parameters, k_Q , g_{sx} , D_0 , Q_{50} , k_A and f .

3.2. Estimation of ET_{RS}

The LAI-based P-M approach was used to estimate 8-day to annual ET_{RS} at 1-km resolution in the 1.1 million km² Murray-Darling Basin (MDB) (Figure 1). To calibrate and test the approach, we obtained 8-day MODIS/Terra-LAI data, annual MODIS/Terra-Land Cover Classification data, daily meteorological data, Digital Elevation Model (DEM), albedo map and daily runoff data.

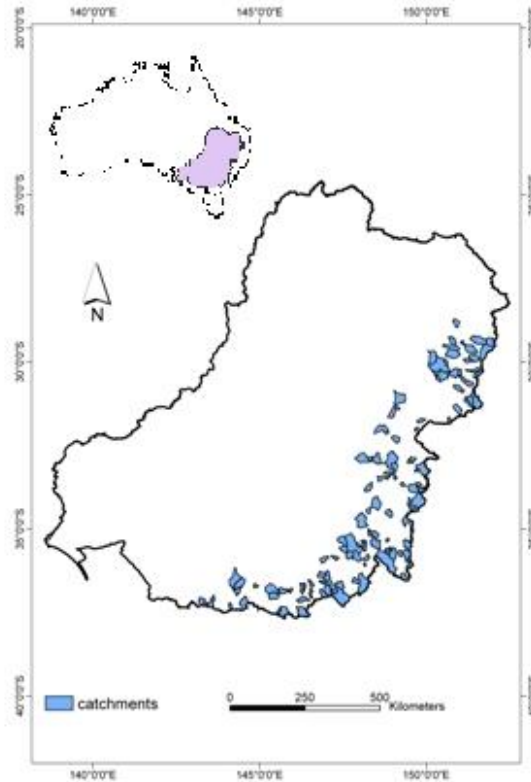


Figure 1. Locations of gauged catchments used in the analyses

The 8-day composite LAI products (MOD15A2) and Land cover classification yearly products (MOD12Q1) were downloaded from the Land Processes Distributed Active Archive Centre (LPDAAC) for the period of 2000-2006. For the pixels assigned as class of settlements and no-

vegetated, LAI was given as a fix value 0.1. LAI was taken as 0 for the water-covered pixels where Priestley-Taylor potential ET replaces ET_{RS} . The Quality Assessment (QA) flags in the LAI dataset were used to keep off bad quality data. Then the deleted data were replaced from the temporal interpolation of good quality data. Gridded daily meteorological data (maximum air temperature, minimum air temperature, vapour pressure, solar radiation and precipitation) were obtained from SILO (<http://www.nrw.qld.gov.au/silo/datadrill/>). The 0.05° ($\sim 5 \text{ km} \times 5 \text{ km}$) SILO gridded data are based on interpolation of point climate observations of the Australian Bureau of Meteorology (BoM). An annual average albedo product at the 5-km resolution for Australia was provided by the BoM.

The above data products were processed by reprojection, subset and resample to obtain the 1-km resolution data across the MDB. To estimate 8-day ET_{RS} , 8-day composite data of maximum and minimum air temperatures, vapor pressure and solar radiation were estimated from the average of the daily corresponding metrological data to match the 8-day MODIS-LAI aggregation period.

3.3. Model calibration

The five parameters, g_{sx} , k_Q , D_0 , Q_{50} and f (k_A was set to 0.7), were calibrated using the generalized pattern search method in MATLAB (Franchini *et al.* 1998). ET_{RS} was calibrated against the mean annual ET derived from water balance estimates separately for catchments in three climate regions: P1, P2 and P3.

In the calibration, the parameters were optimized against the Nash-Sutcliffe Efficiency coefficient (E) (Nash and Sutcliffe 1970), defined as:

$$F = 1 - E = \frac{\sum_{i=1}^N (R_{obs,i} - R_{sim,i})^2}{\sum_{i=1}^N (R_{obs,i} - \bar{R}_{obs})^2} \quad (9)$$

E describes the agreement between the simulated (R_{sim}) and observed (R_{obs}) values, with $E = 1.0$ indicating that all the modelled values are the same as the observed values. \bar{R}_{obs} is the arithmetic mean of the observed values and \bar{R}_{sim} is the arithmetic mean of the modelled values.

The optimized parameter values are shown in Table 1. The optimized values of g_{sx} and D_0 are similar in the three climatic regions. The parameter f is lower in the drier region and Q_{50} is higher in the drier region.

Table 1. Optimized parameter values for the G_s model in three climate regions: P1 ($P < 750$); P2 ($450 \leq P \leq 750$); and P3 ($P > 450$) (P is in mm).

Symbol	Unit	P1	P2	P3
g_{sx}	m/s	0.0047	0.0047	0.0045
k_Q	-	0.53	0.80	0.59
Q_{50}	MJ/m ² /d	2.3	0.45	0.27
D_0	kPa	0.7	0.7	0.7
f	-	0.51	0.45	0.27
k_A	-	0.7	0.7	0.7

4. RESULTS AND DISCUSSION

Figure 2 compares the estimates of mean annual ET_{RS} for the 76 catchments (averaged over 2001-2005) in eastern MDB with the water balance ET (ET_{WB}) estimates. The mean annual ET_{RS} compared well with mean annual ET_{WB} with root mean square error (RMSE) of 65 mm/yr and E of 0.73, indicating that the MODIS-based P-M approach can satisfactorily estimate catchment scale ET. Note that the accuracy of ET_{RS} does not depend on size or location of the 76 catchments.

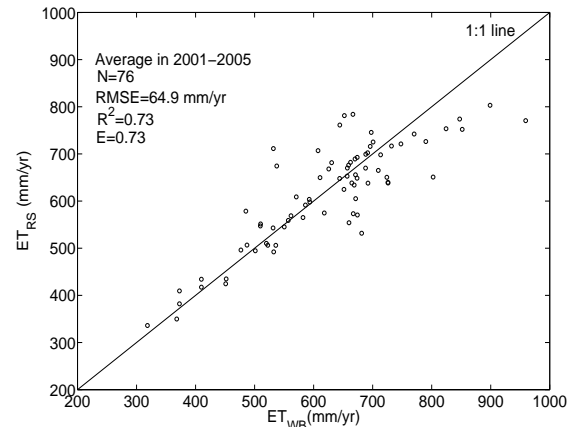


Figure 2. Comparison of mean annual ET_{RS} and ET_{WB}

Figure 3 shows the spatial distribution of ET_{RS} across the MDB. There is a clear east to west gradient, with much higher ET_{RS} in the east because annual precipitation considerably decreases from the east to the west. ET_{RS} also shows high spatial resolution and heterogeneous spatial pattern, which is accordant to a heterogeneous vegetation cover. From the eastern to middle and to western MDB, vegetation changes from forests to crops and shrubs. It is also expected ET_{RS} is better fitted in the east since the calibration is carried out according to eastern gauged catchments (Figure 1). It is difficult to

evaluate the accuracy of ET_{RS} in western and middle parts due to non-gauged catchments there.

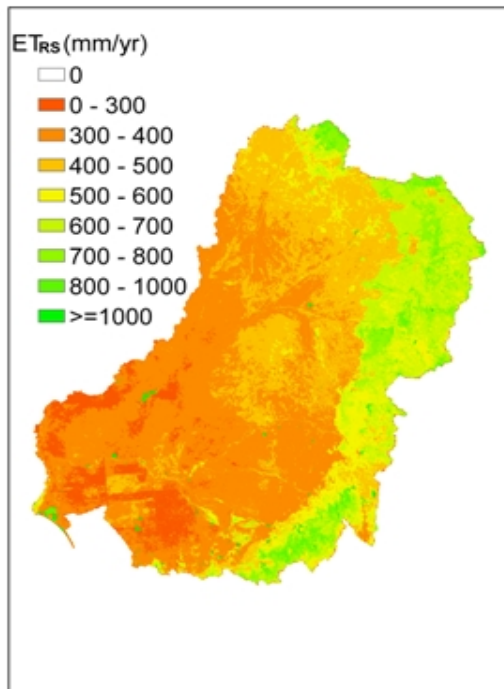


Figure 3. Spatial pattern of ET_{RS} across MDB (mean annual values averaged over 2001-2005)

The potential for using ET_{RS} to estimate long-term runoff at ungauged catchments was also examined by comparing runoff from the water balance estimates ($R_{RS}=P-ET_{RS}$) (mean annual value averaged over 2001-05) with the recorded runoff at the 76 gauged catchments (see Figure 4). The comparisons indicate that R_{RS} matches the recorded runoff reasonably well, with an RMSE of 57.9 mm and E of 0.73. (Note that R_{RS} was set to 0 when ET_{RS} is greater than the mean annual rainfall). The influences of lateral groundwater flow on R_{RS} are negligible because R_{RS} was aggregated in each catchment. The current results are inspiring. It suggests that ET_{RS} can be used to estimate long-term runoff.

It would be interesting to compare R_{RS} estimates for ungauged catchments with those derived from regionalized rainfall-runoff models or other large-scale water balance methods (e.g., Budyko curves), to explore the use of remote sensing to estimate runoff in ungauged catchments.

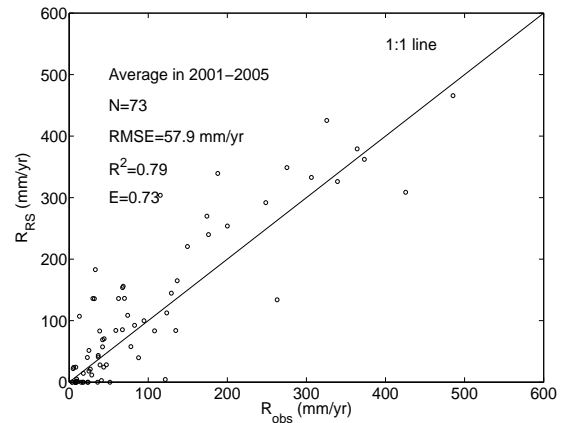


Figure 4. Comparison of mean annual runoff estimates as rainfall minus ET_{RS} with recorded one

5. CONCLUSIONS

The results indicate that the MODIS-based Penman-Monteith approach can satisfactorily estimate catchment scale ET. The results also suggest that the approach can reasonably estimate catchment runoff. This is particularly interesting because the approach used here is relatively simple and requires only routine meteorological data and MODIS-LAI as input data. The remote sensing based ET estimates also provide spatial coverage over entire regions of interest (e.g. entire Murray-Darling Basin or Australia).

It is likely that the approach used here and other remote sensing based ET methods can be used together with rainfall-runoff models (either to constrain rainfall-runoff model estimates or to improve rainfall-runoff model calibration, parameterization and regionalisation) to improve runoff predictions in ungauged catchments. Research on these is ongoing and will be published in subsequent papers.

6. REFERENCES

- Bastiaanssen, W. G. M., E. J. M. Noordman, H. Pelgrum, G. Davids, B. P. Thoreson, and R. G. Allen (2005), SEBAL model with remotely sensed data to improve water-resources management under actual field conditions, *Journal of Irrigation and Drainage Engineering-Asce*, 131, 85-93.
- Cleugh, H. A., R. Leuning, Q. Z. Mu, and S. W. Running (2007), Regional evaporation estimates from flux tower and MODIS satellite data, *Remote Sensing of Environment*, 106, 285-304.

- Franchini, M., G. Galeati, and S. Berra (1998), Global optimization techniques for the calibration of conceptual rainfall-runoff models, *Hydrological Sciences Journal-Journal Des Sciences Hydrologiques*, 43, 443-458.
- Leuning, R., Y. Q. Zhang, Rajaud A., and H. A. Cleugh (2007), A simple surface conductance model to estimate evaporation using MODIS leaf area index and the Penman-Monteith equation *Water Resources Research*, submitted.
- Monteith, J. L., and M. H. Unsworth (1990), *Principles of Environmental Physics.*, 2nd edn., Edward Arnold, London, 291 pp.
- Nash, J. E., and J. V. Sutcliffe (1970), River forecasting using conceptual models, 1. A discussion of principles, *Journal of Hydrology*, 10, 280-290.
- Zhang, L., and W. R. Dawes (1995), Influence of atmospheric stability upon evapotranspiration estimates - tests using HAPEX-MOBILHY data and the WAVES model. CSIRO, Division of Water Resources Technical Memorandum, 95/1.
- Zhang, Y. Q., and M. Wegehenkel (2006), Integration of MODIS data into a simple model for the spatial distributed simulation of soil water content and evapotranspiration, *Remote Sensing of Environment*, 104, 393-408.